J. of Basic Sciences, Cheju Nat'l Univ
14(2) 53~58 2001

기초과학연구 제주대학교
14(2), 53~58, 2001

Analysis of $^{12}C+^{12}C$ Elastic Scattering at $E_{lab}=240$ MeV by Using a First-Order Eikonal Phase Shift

Yong Joo Kim and Hye Young Moon

Department of Physics and Research Institute for Basic Sciences, Cheju National University, Jeju 690-756

The elastic scattering of $^{12}C+^{12}C$ system at $E_{lab}=240$ MeV have been analyzed by using the first-order eikonal phase shift based on Coulomb trajectories of collding nuclei and squared Woods-Saxon potential. The calculated results lead to a reasonable agreements with the observed data of this system. The Fraunhöfer oscillations observed in the elastic angular distributions of the $^{12}C+^{12}C$ system at $E_{lab}=240$ MeV could be explained due to the interference between the near- and far-side scattering amplitudes. The presence of nuclear rainbow is evidenced through the classical deflection function. The refractive pattern, dominated by the far-side component of the scattering amplitude, could be shown to be sensitive to the real part of optical potential at small radii. We have found that the first-order eikonal effect on the imaginary potential is important when the real potential is strong and the imaginary potential is weak.

I. INTRODUCTION

The elastic scattering between heavy-ions has been studied by a number of people using a variety of theoretical methods [1-8]. The heavy-ion elastic scattering is generally dominated by the strong absorption, which the implication that the data are only sensitive to the surface of the interaction region. Therefore, the optical potential required to describe the measurements is not uniquely determined. However, the angular distribution for lighter heavy-ion elastic scattering such as $^{12}C + ^{12}C$ and $^{16}O + ^{16}O$ systems has shown the presence of strong refractive effects with a clear signature of a nuclear rainbow phenomena [1,2]. Such a behavior was identified as being a typical refraction effect generated by the nuclear rainbow. The nuclear rainbows seen in the elastic scattering angular distributions of lighter heavy-ion systems unambiguously determine the major features of the optical potential.

In recent, there has been a great deal of studies to describe the lighter heavy-ion elastic scattering. Shallow imaginary potentials are found to be essential to describe various sets of elastic scattering data for $^{12}C + ^{12}C$ and $^{16}O + ^{12}C$ at intermediate energies [1]. Brandan and McVoy [5] made a systematic study of the optical potentials for lighter heavy-ions. They made several interesting observations, especially on the characteristics of the ratios of the imaginary to real parts of the potentials and of the imaginary to real parts of the phase shifts. The experimental data on elastic $^{16}O + ^{16}O$ scattering at incident energies ranging from 124 to 1120 MeV have been analyzed within the standard optical model, using either the phenomenological potential or that calculated within the double-folding model for the real part of the optical potential [8].

Over the past several years, the eikonal approximation [9] has been a useful tool to describe the heavy-ion elastic scattering. A number of studies [10-14] have been made to describe the elastic scattering processes between heavy ions within the framework of the eikonal model. In a recent paper[15], we have presented the first- and second-order corrections to the zero-order eikonal phase shifts for heavy-ion elastic scatterings based on Coulomb trajectories of colliding nuclei and it has been applied satisfactorily to the $^{16}O + ^{40}Ca$ and $^{16}O + ^{90}Zr$ systems at $E_{lab}=1503$ MeV. Eliseev and Hanna [6] have developed first- and third-order non-eikonal corrections to the Glauber model to know the possibility of observing a bright interior in the nucleus "viewed" by intermediate energy alpha particles ($E_\alpha=172.5$ MeV), as a probe for the ^{58}Ni nucleus. Aguiar *et al.* [14] have discussed different schemes devised to extend the eikonal approximation to the regime of low bombarding energies in heavy-ion collisons. The elastic scatterings of $^{12}C + ^{12}C$ system at E_{lab} = 240, 360 and 1016 MeV are analyzed using the first-order eikonal model [16].

In this work, we analyze the elastic scattering angular distributions of the $^{12}C + ^{12}C$ system at $E_{lab}=240$ MeV by using the first-order eikonal phase shift and Woods-Saxon squared potential. The presence of nuclear rainbow is examined. We also investigate some features of the effective optical potential and phase shift. In section II, we present the theory related with first-order eikonal model. Section III contains the results and discussions. Finally, conclusions are presented in section IV.

II. THEORY

If there is a single turning point in the radial Schrödinger equation, a WKB expression for the nuclear elastic phase shifts δ_L, taking into account the deflection

effect due to Coulomb field, can be written as [17]

$$\delta_L = \int_{r_t}^{\infty} k_L(r)\,dr \; - \int_{r_C}^{\infty} k_C(r)\,dr, \qquad (1)$$

where r_t and r_C are the turning points corresponding to the local wave numbers $k_L(r)$ and $k_C(r)$ given by

$$k_L(r) = k\Big[1 - \Big(\frac{2\eta}{kr} + \frac{(L+\frac{1}{2})^2}{k^2r^2} + \frac{U(r)}{E}\Big)\Big]^{1/2}, \qquad (2)$$

$$k_C(r) = k\Big[1 - \Big(\frac{2\eta}{kr} + \frac{(L+\frac{1}{2})^2}{k^2r^2}\Big)\Big]^{1/2}, \qquad (3)$$

where η is the Sommerfeld parameter, and $U(r)$ the nuclear potential. If we consider the nuclear potential as a perturbation, the turning point r_t may be taken to be coincident with the distance of closest approach r_C given by

$$r_C = \frac{1}{k}\Big\{\eta + \Big[\eta^2 + (L+\frac{1}{2})^2\Big]^{1/2}\Big\}. \qquad (4)$$

Thus, the nuclear phase shift δ_L in Eq.(1) can be rewritten

$$\delta_L = -\frac{\mu}{\hbar^2}\int_{r_C}^{\infty}\frac{U(r)}{k_C(r)}dr - \frac{\mu}{2\hbar^4}\int_{r_C}^{\infty}\frac{U^2(r)}{k_C^3(r)}dr \qquad (5)$$

where $r = \sqrt{r_C^2 + z^2}$, μ is the reduced mass.

The first term in Eq.(5) is the ordinary Coulomb-modified eikonal phase shift function, while the second term is the first-order corrections correspond to non-eikonal effects. The expressions of each terms in Eq.(5) are explicitly[15]

$$\delta_L^0(r_C) = -\frac{\mu}{\hbar^2 k}\int_0^{\infty} U(r)\,dz, \qquad (6)$$

$$\delta_L^1(r_C) = -\frac{\mu^2}{2\hbar^4 k^3}\Big(1 + r_C\frac{d}{dr_C}\Big)\int_0^{\infty} U^2(r)\,dz. \qquad (7)$$

The first-order eikonal correction term of the phase shift, $\delta_L^1(r_C)$ in Eq.(7), can further be expressed as following

$$\delta_L^1(r_C) = -\frac{\mu^2}{\hbar^4 k^3}\int_0^{\infty}\Big[U^2(r) + rU(r)\frac{dU(r)}{dr}\Big]\,dz\,. \qquad (8)$$

The closed expression of the effective phase shift function including up to the first-order correction term may be written as

$$\delta_L(r_C) = -\frac{\mu}{\hbar^2 k}\int_0^{\infty} U_{\rm eff}(r)\,dz\,, \qquad (9)$$

where $U_{\rm eff}(r)$ is the effective optical potential given by

$$U_{\rm eff}(r) = U\Big\{1 + \frac{\mu}{\hbar^2 k^2}\Big[U + r\frac{dU}{dr}\Big]\Big\}. \qquad (10)$$

We can see that the phase shift calculation including non-eikonal corrections up to the first-order is equivalent to a zeroth-order calculation with effective potential $U_{\rm eff}(r)$.

By taking $U(r)$ as the squared Woods-Saxon forms given by

$$U(r) = -\frac{V_0}{(1+e^{(r-R_v)/a_v})^2} - i\frac{W_0}{(1+e^{(r-R_w)/a_w})^2}, \qquad (11)$$

with $R_{v,w} = r_{v,w}(A_1^{1/3} + A_2^{1/3})$, we can use the phase shift, Eq.(9) in the general expression for the elastic differential scattering cross section. The elastic differential cross section between two identical spinless nuclei can be obtained from the following formula

$$\frac{d\sigma}{d\Omega} = |f(\theta) + f(\pi - \theta)|^2, \qquad (12)$$

where elastic scattering amplitude $f(\theta)$ is given by the equation

$$f(\theta) = f_{\rm R}(\theta) + \frac{1}{ik}\sum_{L=0}^{\infty}(L+\frac{1}{2})\exp(2i\sigma_L)(S_L^{\rm N} - 1)P_l(\cos\theta)\,. \qquad (13)$$

Here $f_{\rm R}(\theta)$ is the usual Rutherford scattering amplitude and σ_L the Coulomb phase shifts. The nuclear S-matrix elements S_L^N in this equation can be expressed by the nuclear phase shifts δ_L

$$S_L^N = \exp(2i\delta_L). \qquad (14)$$

III. RESULTS AND DISCUSSIONS

The elastic differential cross sections for ^{12}C + ^{12}C system at $E_{\rm lab}$= 240 MeV are calculated by using the Coulomb-modified eikonal phase shifts δ_L^0 and δ_L^1. Table 1 shows the parameters of the fitted Woods-Saxon squared potential. The six potential parameters are adjusted so as to minimize the χ^2/N given by

$$\chi^2/N = \frac{1}{N}\sum_{i=1}^{N}\left[\frac{\sigma_{exp}^i - \sigma_{cal}^i}{\triangle\sigma_{exp}^i}\right]^2. \qquad (15)$$

In Eq.(15), σ_{exp}^i (σ_{cal}^i) and $\triangle\sigma_{exp}^i$ are the experimental (calculated) cross sections and uncertainties, respectively, and N is the number of data used in the fitting. The calculated results of the differential cross sections for the elastic scattering of ^{12}C + ^{12}C system at $E_{\rm lab}$= 240 MeV is presented in Fig.1 together with those measured experimentally [18]. In this figure, the dashed curve is the result for zero-order eikonal phase shift, while the solid curve is the one of first-order eikonal phase shift. As seen in this figure, the differences between the dotted and solid curves are substantial when compared with the experimental data. As the figure shows, the results of the first-order correction are more reasonable and give

TABLE I: Parameters of the fitted Woods-Saxon squared potential by using the first-order eikonal model analysis for the ^{12}C + ^{12}C elastic scattering at E_{lab}= 240 MeV. 10 % error bars are adopted to obtain χ^2/N value.

V_0 (MeV)	r_v (fm)	a_v (fm)	W_0 (MeV)	r_w (fm)	a_w (fm)	R_S (fm)	σ_{R_S} (mb)	σ_R (mb)	χ^2/N δ^0	$\delta^0+\delta^1$
323	0.636	1.768	24.5	1.258	1.010	6.39	1283	1334	10.45	4.99

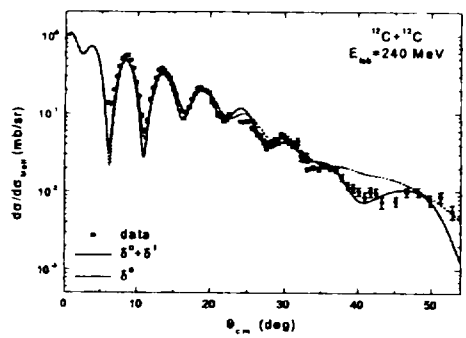

FIG. 1: Elastic scattering angular distributions for ^{12}C + ^{12}C system at E_{lab}= 240 MeV. The solid circles denote the observed data taken from Ref.[18]. The solid and dashed curves are the results for first- and zeroth-order eikonal corrections, respectively.

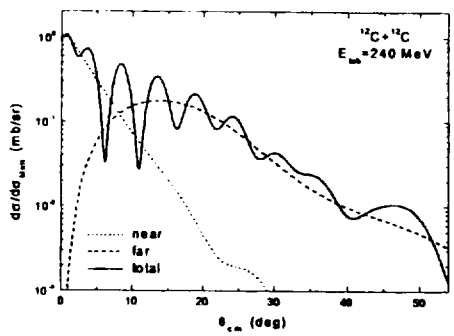

FIG. 2: Differential cross section (solid curves), near-side contribution (dotted curves), and far-side contribution (dashed curves) obtained by the Fuller's formalism [19] using the first-order eikonal model for ^{12}C + ^{12}C system at E_{lab}= 240 MeV.

better fits with the observed data than the results from the zeroth-order correction. Also, the reasonable χ^2/N values is obtained in the ^{12}C + ^{12}C system at E_{lab}= 240 MeV as listed in table 1. In the Table 1, R_S is the strong absorption radius. The strong absorption radius is defined as the distance for which T_L = 1/2, i.e., the distance where the incident particle has the same probability to be absorbed as to be reflected. The strong absorption radius provides a good estimate of the reaction cross section, $\sigma_{R_S} = \pi R_S^2$.

More insight into the diffractive and refractive phenomena can be provide by the representation of the elastic scattering amplitude in terms of the near-side and far-side component. The near- and far-side decompositions of scattering amplitudes with the first-order correction to the eikonal phase shifts are performed by following Fuller's formalism [19]. The contributions of the near- and far-side components to the elastic scattering cross sections are shown in Fig. 2 along with the differential cross section. The differential cross section is not just a sum of the near- and far-side cross sections but contains the interference between the near- and far-side amplitudes as shown in Fig. 2. The refractive oscillation observed on the elastic scattering angular distribution of ^{12}C + ^{12}C system at E_{lab}=240 MeV is due to the interference between the near- and far-side components. The magnitude of the near- and far-side contributions is equal, crossing point, at $\theta = 8.1°$ for this reaction. This figure shows the near-side dominance at angles less than this value due to the long-range repulsive Coulomb interaction. However, the far-side scattering has become dominant at the regions greater than the crossing angle due to the short-range attractive nuclear interaction.

The transmission function $T_L = 1-|S_L|^2$ is plotted versus the orbital angular momentum in Fig.3, along with the deflection function. The transmission function can be explained using the imaginary part of the effective optical potential. As shown Fig. 3(a), the lower partial waves are totally absorbed and the T_L is decreased very rapidly in a narrow localized angular momenta zone. The strongly refractive- and weakly absorptive-potential values are enough to support nuclear rainbow. As shown in table 1, the absorption in ^{12}C + ^{12}C system is weak enough to allow refracted projectiles to populate the elastic channel and typical nuclear effects could be observed in the angular distribution. The presence of nuclear rainbow can be proved by investigating the deflection function given by $\theta_L = 2\frac{d}{dL}(\sigma_L + \mathrm{Re}\ \delta_L)$. In a rainbow situation, the strong nuclear force attracts the projectiles towards the scattering center and deflects them to negative angle, which correspond to the region of the rainbow maximum. In Fig. 3(b), we can find the nuclear rainbow

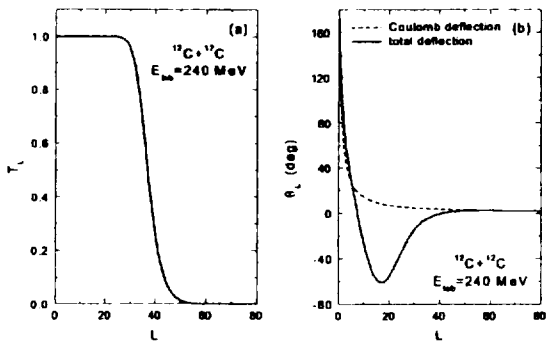

FIG. 3: (a) Transmission function T_L and (b) deflection function for ^{12}C + ^{12}C system at E_{lab}= 240 MeV plotted versus the orbital angular momentum L in the first-order eikonal model. The dashed curve represents the deflection function for the Coulomb phase shift.

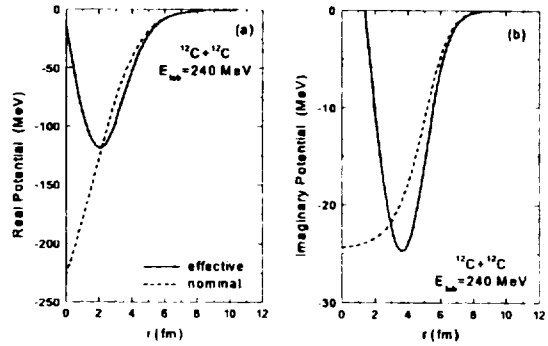

FIG. 4: (a) Real and (b) imaginary parts of the effective potential for the ^{12}C + ^{12}C system at E_{lab}= 240 MeV. The solid and dashed curves are the results for the first- and zeroth-order eikonal corrections, respectively.

angle value $\theta_{nr} = -60.6°$, which evidently prove a presence of the nuclear rainbow with unambiguous clarity in this system.

In Fig.4, we plot the real and imaginary parts of effective potential in Eq.(10) and nominal potential in Eq.(11), and examine the effect of first-order non-eikonal correction. Figure 4(a) and 4(b) present the real and imaginary part of optical potential, respectively. The solid curves are the first-order effective potentials $U_{\rm eff}(r)$ given by Eq.(10), while the dashed curves are the results of nominal potential $U(r)$. As shown in this figure, there is a dramatic difference between the two potentials, especially for the imaginary part. We can see in Eq.(10) that the effective imaginary potential with the first-order eikonal correction depends on the product of the real and imaginary potentials and their derivatives. Thus the effective imaginary potentials rapidly increase until they reach maximum value in the central region of the nucleus, and then they reach minimum in the surface region. A drastic increase of the imaginary potential for small values of r corresponding to increased transmission is mainly due to the correction term in Eq.(10). In the traditional optical model, it is assumed that the imaginary part of the potential is responsible for the absorption process in the nuclear reaction and its shape should not be affected by the real part. Nevertheless, in the present eikonal model with the first-order correction, we can find that the drastic increase on the absorptive potential in the small r region are due to the larger real potential compared with imaginary one. In the small r region, the effective imaginary potential of the first-order eikonal model is small compared with the effective real potential. As a result the projectile ion can penetrate the nuclear surface barrier of the target, and the cross section becomes sensitive to the value of the real potential in the central region.

As is well-known, a behavior of the effective potential in the small r region is reflected in the phase shift function. Figure 5 shows angular momentum dependence of the real and imaginary parts of the eikonal phase shifts. The solid curves are the first-order eikonal model, while the dashed curves are the results of the ordinary eikonal model. The real phase shift vanishes nearly quadratically as the L increases. The real phase shift of the first-order eikonal corrections is less values than the result of zeroth-order eikonal phase shift at $L < 7$ and, however, is greater ones than one of zeroth-order case at $L > 7$. On the other hand, we can find the dramatic variations of the imaginary phase shifts for this system, as expected. The strong absorption in the nuclear surface plays a dominant role to the scattering amplitude and thus to the characteristic diffraction pattern of the angular distribution. The large angle behavior is sensitive to the details of the real optical potential over a wide radial region from the nuclear surface towards the interior.

IV. CONCLUSIONS

In this work, we have analyzed the elastic scattering of ^{12}C+ ^{12}C system at E_{lab}=240 MeV by using the first-order eikonal model based on the Coulomb trajectories of colliding nuclei and squared Woods-Saxon potential. We have found that the calculated results using the first-order eikonal model are in reasonable agreement with the observed data. Through near- and far-side decompositions of the cross section, we have shown that near-side dominates at forward angles, and the refractive oscillation of this system is due to the interference between the

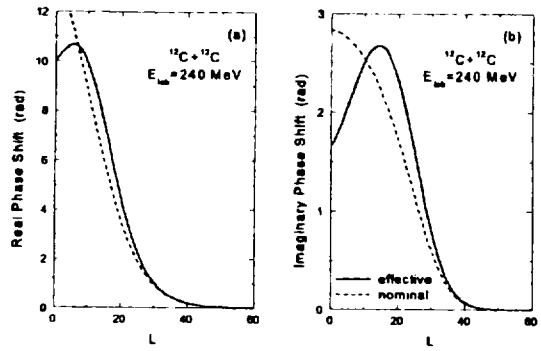

FIG. 5: (a) Real and (b) imaginary part of the effective phase shift for the ^{12}C + ^{12}C system at E_{lab}= 240 MeV. The solid and dashed curves are the results for the first- and zeroth-order eikonal corrections, respectively.

near- and far-side amplitude. The elastic scattering pattern at large angles was dominated by the refraction of the far-side trajectories. The presence of a nuclear rainbow is also evidenced by the classical deflection function.

The strongly real and weakly imaginary optical potentials are found and they support the presence of nuclear rainbows in the angular distribution of this system. We have also found that the effect of first-order eikonal correction on the imaginary potential is important in this case. The strong real potential give a drastic effect on the effective imaginary potential for ^{12}C + ^{12}C system at E_{lab}= 240 MeV. The refractive part, dominated by the far-side component of the scattering amplitude, is sensitive to the real heavy-ion optical potential at small radii. The imaginary effective potential of first-order eikonal model have pronounced minimum between central and surface regions of nucleus, while the nominal imaginary potential increase monotonically. Such a effective potential is reflected in the phase shift function. The strongly real potential gives a drastic effect on the imaginary phase shift for ^{12}C + ^{12}C system at E_{lab}= 240 MeV. We can also see in the imaginary phase shift calculated with the real potential that an absorption of partial waves for large angular momentum increases, whereas the absorption decreases for small angular momentum, compared to the result without the real potential. The strong absorption in the nuclear surface plays a dominant role to the scattering amplitude and thus to the characteristic diffraction pattern of the angular distribution. The large-angle behavior is sensitive to the details of the real optical potential over a wide radial region from the nuclear surface towards the interior.

REFERENCES

[1] M. E. Brandan, Phys. Rev. Lett. **60**, 784 (1988).

[2] E. Stiliaris, H. G. Bohlen, P. Fröbrich, B. Gebauer, D. Kolbert, W. von Oertzen, M. Wilpert and Th. Wilpert, Phys. Lett. **223**, 291 (1989).

[3] A. Ingemarsson and G. Fäldt, Phys. Rev. C **48**, R507 (1993)

[4] M. E. Brandan, H. Chehime and K. W. McVoy, Phys. Rev. C **55**, 1353 (1997)

[5] M. E. Brandan and K. W. McVoy, Phys. Rev. C **55**, 1362 (1997)

[6] S. M. Eliseev and K. M. Hanna, Phys. Rev. C **56**, 554 (1997).

[7] A. Ingemarsson, Phys. Rev. C **56**, 950 (1997)

[8] Dao T. Khoa, W. von Oertzen, H. G. Bohlen and F. Nuoffer, Nucl. Phys. **A672**, 387 (2000).

[9] D. Waxman, C. Wilkin, J. -F. Fermond and R. J. Lombard, Phys. Rev. C **24**, 578 (1981).

[10] T. W. Donnelly, J. Dubach and J. D. Walecka, Nucl. Phys. Nucl. Phys. **A232**, 355 (1974).

[11] J. Knoll and R. Schaeffer, Ann. Phys. (N.Y.) **97**, 307 (1976).

[12] R. da Silveira and Ch. Leclercq-Willain, J. Phys. G **13**, 149 (1987).

[13] G. Fäldt, A. Ingemarsson and J. Mahalanabis, Phys. Rev. C **46**, 1974 (1992).

[14] C. E. Aguiar, F. Zardi and A. Vitturi, Phys. Rev. C **56**, 1511 (1997).

[15] M. H. Cha and Y. J. Kim, Phys. Rev. C **51**, 212 (1995).

[16] Y. J. Kim, M. H. Cha, Int. J. Mod. Phys. **E9**, 67 (2000).

[17] C. K. Chan, P. Suebka and P. Lu P, Phys. Rev. C**24**, 2035 (1981).

[18] H. G. Bohlen, X. S. Chen, J. G. Cramer, P. Fröbrich, B. Gebauer, H. Lettau, A. Miczaika, W. von Oertzen, R. Ulrich and T. Wilpert, *Z. Phys.* **322** (1985) 241.

[19] R. C. Fuller, Phys. Rev. C **12**, 1561 (1975).

제1차 Eikonal 위상이동을 이용한 $E_{lab}=240MeV$에서의 $^{12}C+^{12}C$ 탄성산란 분석

김용주, 문혜영
제주대학교 물리학과, 기초과학연구소, 제주 690-756

요 약

$E_{lab}=240MeV$에서의 $^{12}C+^{12}C$ 탄성산란을 쿨롱궤적에 기초한 제1차 Eikonal 위상이동과 제곱형 Woods-Saxon 퍼텐셜을 이용하여 분석하였다. 계산결과는 실험값과 좋은 일치를 보여주었다. $E_{lab}=240MeV$에서 $^{12}C+^{12}C$계의 탄성산란 각분포에서 관측된 Fraunhöfer 진동은 원측과 근측 산란진폭의 간섭현상으로 설명될 수 있었다. 고전적 편향함수로부터 핵 무지개 현상의 존재를 알 수 있었다. 원측 산란진폭이 중요한 역할을 하는 굴절성 패턴은 작은거리에서의 광학 퍼텐셜의 실수부에 민감함을 알 수 있었다. 실수 퍼텐셜이 강하고 허수 퍼텐셜이 약할 때 허수 퍼텐셜에 대한 제1차 Eikonal 효과는 매우 중요함을 알 수 있었다.